Available online at www.sciencedirect.com
ScienceDirect
European Journal of Mechanics B/Fluids 27 (2008) 239–250

Chaotic stirring in a new type of mixer with rotating rigid blades

Tzong-Yih Hwu *

Department of Computer Application Engineering, LanYang Institute of Technology, No 79, FuShin Rd., TouCheng, I-Lan Hsien 261, Taiwan

Received 13 December 2006; received in revised form 2 May 2007; accepted 8 May 2007

Available online 23 May 2007

Abstract

The present study suggests a new conceptual apparatus that can be used to stir fluids at low velocities. This consists of a circular container equipped with one or two blades arranged along the perimeter which drive the fluid motion. It modifies a previous apparatus in which fluid was driven by two flexible belts, which is more difficult to implement in experiments. Using the new device, fluid can be stirred completed with very high fluid stretch-rates in a short time. This could not be obtained in the previous studies by the belts. Based on extensive computations, the greatest averaged fluid stretch-rate is created by rotating two blades of lengths $3\pi/4$ and $\pi/2$, with the second blade actuated at a frequency ten times higher than the first blade. When only one blade is employed, shorter periods are beneficial to stirring of fluid and produce higher fluid stretch-rates.

Keywords: Fluid mixer; Blade; Circular container; Averaged fluid stretch-rate

1. Introduction

In the last two decades, a large number of studies have been devoted to stirring of fluid. These studies have been motivated by the physical interest of the problem, as well as a variety of applications. What is stirring of fluid? Simply speaking, it consists of agitating fluid by using some moving boundaries that can be set outside or inside fluid domains. Due to the stirring action, any two fluid particles or blobs which are initially located far from to each other may rapidly find themselves close to each other. Stirrings of fluid have various applications, for example, in material processing, food engineering, chemical engineering, and in biomedical engineering. Rather than use turbulent flows or other mechanisms requiring higher velocities, a complete stirring of fluid can be obtained in laminar flows or even in the limit of Stokes flows. Gentle stirring is particularly important for fluids consisting of long molecules. For such fluids, velocities at which fluid is deformed must not be too high to avoid destroying the structure of the fluid molecules. Therefore stirrings of fluid are frequently performed in the Stokes flow regime.

To clearly understand stirring processes of fluid, experimental, theoretical and numerical efforts are equally necessary. As fluid moves very slowly, theoretical and numerical treatments are relatively simpler than those for flows at higher velocities. Furthermore, the results obtained by the three distinct methods can be compared with each other in great detail. This is nearly impossible to do for fluid transported at high velocities. Therefore, the study for the stirring

* Correspondence address: No 20, Alley 2, Min-Chu Lane 2, Tai-Shan Rd., I-Lan City, I-Lan Hsien 260, Taiwan. Tel.: +886 3 9771997ext 260; fax: +886 2 29303414.
E-mail address: tyhwu@mail.fit.edu.tw.

0997-7546/$ – see front matter
doi:10.1016/j.euromechflu.2007.05.002

of fluid in Stokes flows provides the simplest setting in which to understand the mechanisms underlying chaotic fluid motions.

Studies focused on stirring in the Stokes flow regime already form a rich body of literature. Flows in two-dimensional, journal bearing flows and rectangular cavity flows have been extensively investigated and successfully used to mix fluids (Ottino [1]). The first apparatus consists of a pair of nested cylinders with the inner cylinder positioned eccentrically with respect to the outer one. Fluid fills the space between the cylinders and is driven by periodically rotating the cylinders (Aref and Balachandar [2], Chaiken et al. [3], Swanson and Ottino [4], Dutta and Chevray [5]). The results show that more complete stirring of fluid is obtained when the cylinders are periodically rotated with angular velocities of longer periods. In another configuration, fluid can be efficiently stirred in a rectangular cavity for which two parallel plates are periodically moved (Chien et al. [6], Leong and Ottino [7], Liu et al. [8]). The results are similar to those in the journal bearing flows. Jana, Tjahjadi and Ottino [9] further examined chaotic fluid mixings in baffled cavity flows having geometries that change periodically. The parameters influencing the fluid mixings include the mixing protocol, baffle size and shapes, geometrical and flow parameters, and details of the baffle motions.

Hwu, Young and Chen [10] studied stirring phenomena of fluid in a circular cavity. Fig. 1 shows their conceptual apparatus, featuring a long circular cylinder with two open sectors along the perimeter. The two sectors are occupied by two flexible belts that can be actuated periodically and drive the fluid moving within the container. Under this arrangement, fluid can be stirred according to various belt actuation protocols. Although the flow patterns generated in a circular cavity and in a rectangular cavity are similar to each other, the circular cavity geometry presents some significant mathematical advantages. Most importantly, the velocity fields of the steady circular cavity flows can be represented in closed form. Moreover, the periodic flows resulting from varying boundary motions can be treated in a quasi-steady manner. Trajectories of fluid particles can thus be accurately obtained by integrating the velocity fields of the transient flows with respect to time. It is well known that when fluid moves in a random manner, particle paths are sensitive to the initial conditions and to the accuracy of the computational procedure. By using analytical solutions of the velocity field, one can guarantee more readily that results reflect true physical chaos rather than numerical chaos. Although results obtained so far for stirring of fluid in a circular cavity are comprehensive, the belt drive apparatus described above is subject to a number of limitations. The apparatus is difficult to construct and operate in practical experiments. The main reason is that the belt has a tensional force which tends to pull it away from the perimeter of the cavity. This pull may be opposed by placing some slender cylinders restraining the belt to its desired geometry (Fig. 2). However these small cylinders will change the boundary configuration and potentially affect the entire fluid flows. This will increase discrepancies between theoretical, numerical, and experimental results.

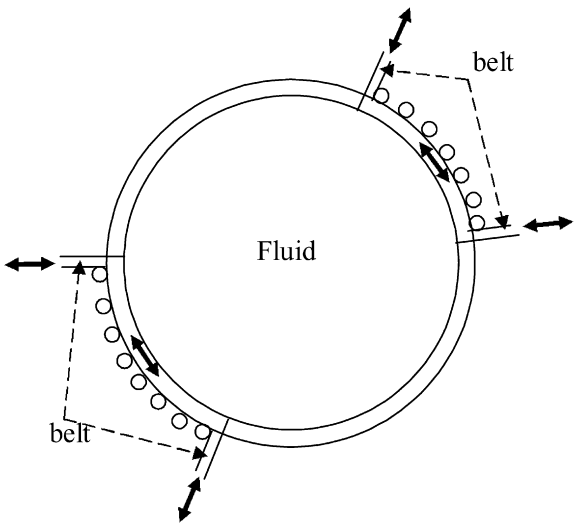

Fig. 1. Sketch of circular cavity with two sliding belts.

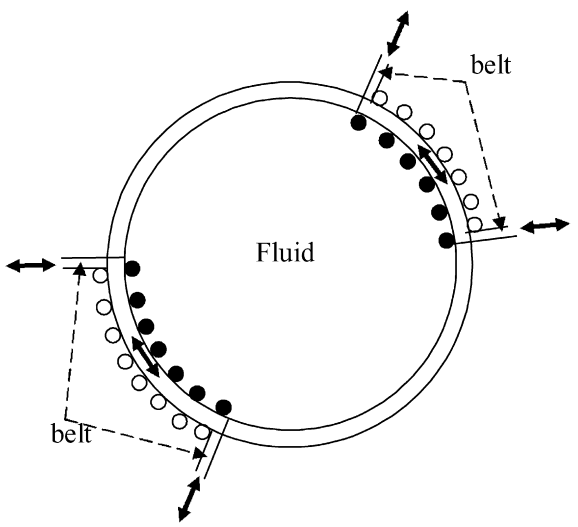

Fig. 2. Sketch of modified circular cavity with some slender cylinders used to constrain the flexible belts.

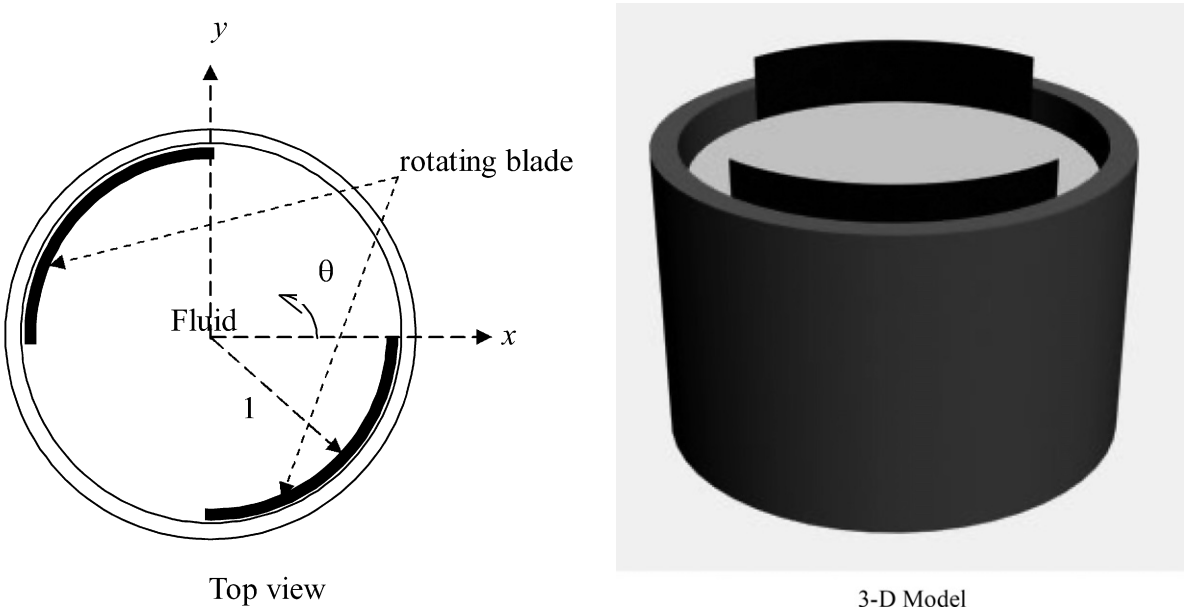

Fig. 3. Sketch of new fluid mixer with one or two rotating blades.

To overcome the shortcoming illustrated above, the present study examines a new configuration featuring rigid blades rotated along the perimeter. This device is again a circular cylindrical container, kept at rest, and two long blades with a circular arc form are installed inside nearly touching the wall of the cylinder (Fig. 3). Fluid within the cylinder is stirred by periodically rotating the two blades. The device is a more realistic apparatus closer to these that can be actually implemented in a laboratory or industrial context. It also permits driving the fluid motions along time-varying sectors of the cavity perimeter, leading to possible gains in stirring efficiency of fluid.

2. Mathematical model

The circular cavity flows treated in the present study are assumed to operate in the Stokes flow regime, hence inertial effects are neglected. As a result, the equations governing the flow field can be reduced to a linear formulation. Furthermore by virtue of Landau's argument [11], the flows can be treated in a quasi-steady manner. It means that when the blades move or change their angular velocities, the velocity of the fluid will be redistributed very quickly throughout the entire cavity. This requires that the time scale needed for redistributing the fluid velocity is much shorter than the time scale governing the motion and angular acceleration of the blades.

Fig. 3 shows a circular cavity with radius of unity and two blades placed inside along the wall of the container. The device is filled with the fluid to be stirred. The parameters controlling the kinematics of the fluid motions are: (1) the lengths of the blades, (2) the initial positions of the blades, (3) the ranges within which the blades are moved, and (4) the protocols of the angular velocities of the rotating blades. The influences of these factors on the stirring of fluid may be very complicated. To allow a systematic exploration, some further simplifications have to be introduced. We restrict our attention to the following cases. The fluid in the container is originally at rest and the two blades are in contact with each other. Then both of the blades are rotated with constant angular velocities and at opposite directions. After each blade has moved, along the boundary through one half of the circle perimeter, it changes its direction of rotation to return to the original position, then repeatedly undertakes such a periodic movement. The periods of oscillation of the two blades can take different values. By restricting blade motions to half of the perimeter, the two blades will not collide and the stirring of fluid will depend only on factors (1) and (4). Moreover, a particular case for which only one blade is rotated is included in the present investigation.

Consider then the velocity field in the circular cavity flow at any given time. The two blades span the following sectors of the boundary: $\alpha_1 \leqslant \theta \leqslant \beta_1, \alpha_2 \leqslant \theta \leqslant \beta_2$ and have angular velocities Ω_1^*, Ω_2^*, respectively. The quasi-steady Stokes flow satisfies the biharmonic equation

$$\nabla^4 \Psi = 0, \tag{1}$$

in which Ψ stands for the stream-function. The corresponding boundary conditions are

$$\Psi = 0 \quad \text{at } r = 1, \tag{2}$$

$$\frac{\partial \Psi}{\partial r} = \begin{cases} -\Omega_1^*, & \alpha_1 \leqslant \theta \leqslant \beta_1, \\ -\Omega_2^*, & \alpha_2 \leqslant \theta \leqslant \beta_2 \end{cases} \quad \text{at } r = 1. \tag{3}$$

The analytical solution of (1)–(3) can be formulated as follows (Tychonov and Samarski [12], Garabedian [13], Mills [14])

$$\Psi = \sum_{i=1}^{2} \frac{(1 - x^2 - y^2)\Omega_i^*}{2\pi} \left\{ \tan^{-1}\left[\frac{(1 + x^2 + y^2 + 2x)\tan \beta_i/2 - 2y}{1 - x^2 - y^2} \right] - \tan^{-1}\left[\frac{(1 + x^2 + y^2 + 2x)\tan \alpha_i/2 - 2y}{1 - x^2 - y^2} \right] \right\}. \tag{4}$$

The time-varying stream-function for the quasi-steady circular cavity flow is then obtained directly by substituting functions $\Omega_i(t)$, $\alpha_i(t)$ and $\beta_i(t)$, yielding

$$\Psi = \sum_{i=1}^{2} \frac{(1 - x^2 - y^2)\Omega_i(t)}{2\pi} \left\{ \tan^{-1}\left[\frac{(1 + x^2 + y^2 + 2x)\tan \beta_i(t)/2 - 2y}{1 - x^2 - y^2} \right] - \tan^{-1}\left[\frac{(1 + x^2 + y^2 + 2x)\tan \alpha_i(t)/2 - 2y}{1 - x^2 - y^2} \right] \right\}. \tag{5}$$

In (5), the periodic rotations of the blades are governed by

$$\Omega_i(t) = \begin{cases} \Omega_i^*, & nT_i < t < (n + 1/2)T_i \\ -\Omega_i^*, & (n + 1/2)T_i < t < (n + 1)T_i \end{cases} \quad (n\text{: an integer; } i = 1, 2) \tag{6}$$

and the two constant angular velocities satisfy $\Omega_1^* \geqslant 0$, $\Omega_2^* \leqslant 0$. Furthermore, the first blade is rotated back and forth along the boundary at the angular velocity $\Omega_1(t)$; T_1 is the corresponding period. The same descriptions apply to the second blade. Because the cavity has unit radius, the lengths of the blades are given by $\beta_i(t) - \alpha_i(t) = L_i \leqslant \pi$. Because each of the blades is constrained to stay within half of the circle, one has $|\Omega_i^*|T_i = 2(\pi - L_i)$. Based on these relations, the position of the first blade appearing in (5) can be written in the more convenient form

$$\alpha_1(t) = \begin{cases} -\pi + \operatorname{mod}(t, T_1)\Omega_1^*, & nT_1 < t < (n + 1/2)T_1, \\ -\operatorname{mod}(t, T_1/2)\Omega_1^* - L_1, & (n + 1/2)T_1 < t < (n + 1)T_1, \end{cases} \tag{7a}$$

$$\beta_1(t) = \alpha_1(t) + L_1 \tag{7b}$$

and, for the second blade,

$$\beta_2(t) = \begin{cases} \pi - \operatorname{mod}(t, T_2)|\Omega_2^*|, & nT_2 < t < (n + 1/2)T_2, \\ \operatorname{mod}(t, T_2/2)|\Omega_2^*| + L_2, & (n + 1/2)T_2 < t < (n + 1)T_2, \end{cases} \tag{8a}$$

$$\alpha_2(t) = \beta_2(t) - L_2. \tag{8b}$$

The blades are initially located at positions $\alpha_1(0) = -\pi, \beta_1(0) = -\pi + L_1$ and $\alpha_2(0) = \pi - L_2, \beta_2(0) = \pi$ at which they are in contact with each other. They are then rotated to drive the fluid. Under the conditions outlined above, the four parameters L_1, L_2, T_1, T_2 control the blade motions and the corresponding fluid responses in the circular cavity. The role of the parameters Ω_1^* and Ω_2^* is accounted for implicitly through relation $|\Omega_i^*|T_i = 2(\pi - L_i)$.

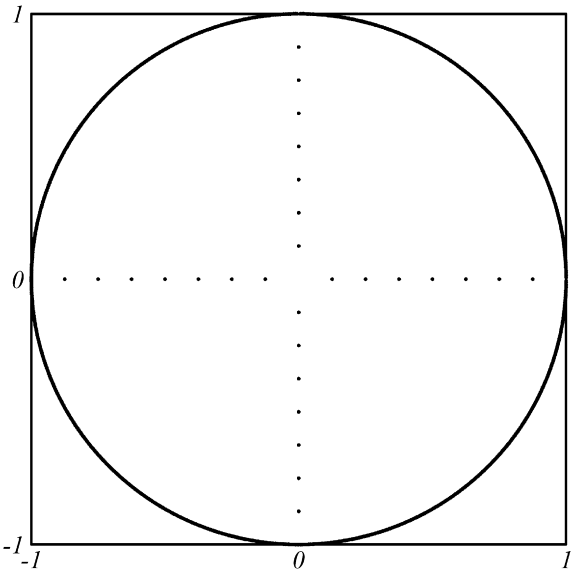

Fig. 4. Initial positions of twenty-eight fluid points used to generate Poincaré sections.

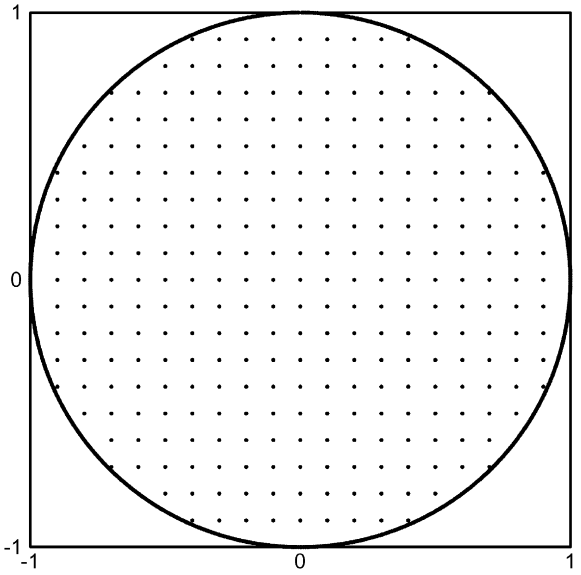

Fig. 5. Initial positions of 305 pairs of fluid filaments employed to compute averaged fluid stretch-rates.

The instantaneous velocity fields associated with the fluid motion can be obtained by taking the derivatives of (5): $\mathrm{d}x/\mathrm{d}t = u = \partial\Psi/\partial y, \mathrm{d}y/\mathrm{d}t = v = -\partial\Psi/\partial x$ and the fluid particle trajectories can be traced by integrating the two velocity components with respect to time. A Runge–Kutta scheme with accuracy of fourth order is used for this purpose. To identify whether fluid experiences chaotic motions and thus whether stirring is indeed achieved, plots of the Poincaré sections and computations of the averaged fluid stretch-rates, abbreviated to AFSR in the present investigation, are invoked (Hwu [15]). Moreover, animations can be produced to illustrate the stirring process of fluid by continuously recording the deformations of some fluid blobs. For plotting the Poincaré sections, 28 fluid points that are initially located as shown in Fig. 4 are traced (Hwu [15]). On the other hand, the AFSR is estimated by the equation $\lambda_{\mathrm{ave}} = \frac{1}{N}\sum_{i=1}^{N}(\lambda_{x,i} + \lambda_{y,i})/2$. In the computations, $N = 305$ pairs of fluid filaments that initially located as shown in Fig. 5 are used (Hwu [15]). $\lambda = d/d_0$ indicates the stretch-rate of a fluid filament of initial length $d_0 = 0.001$ stretched to length d. For each pair of fluid filaments, λ_x and λ_y denote the stretch-rates of the fluid filaments that are initially aligned parallel to x-axis and to y-axis, respectively.

3. Results and discussion

Figs. 6–9 shows the time evolutions of AFSRs in flows driven by blades of various lengths. In each of the plots, the values of L_1 and L_2 are specified. The period T_1 is fixed to be unity and T_2 varies from 0.1 to 1 by increments of 0.1. The total time interval of the computations is 5. Fig. 6 displays the AFSRs generated in the circular cavity with $L_1 = \pi/4$ and $L_2 = \pi/4$. The AFSRs grow as time proceeds. At a given time, the values decrease when period T_2 is increased. The similar results obtained when increasing L_2 from $\pi/4$ to $\pi/2$ are illustrated in Fig. 7. The values of AFSRs are greater than those obtained in the previous case. When the second blade has length $L_2 = 3\pi/4$, the AFSRs decrease as shown in Fig. 8. Fig. 9 demonstrates a particular case with $L_2 = \pi$. In this case, the corresponding blade is kept at rest and the fluid is driven by the other blade with the period of 1. In this situation, the evolutions of the AFSRs dramatically change and the values decrease significantly. When the mixer blades have lengths $L_1 = \pi/2$, $L_1 = 3\pi/4$ and $L_1 = \pi$, the results are similar to those obtained for length $L_1 = \pi/4$.For the cavities with $L_1 = \pi$, the fluid is moved by rotating only one blade but with the period 0.1. Based on these results, higher AFSRs can still be obtained in cavity flows for which only one blade is rotated, provided that the blade is actuated with a shorter period.

Table 1 summarizes the AFSRs that are produced by the cavities with various values of parameters L_1, L_2 and with $T_1 = 1, T_2 = 0.1$. All of the fluid stretching are examined at $t = 5$. The tabulated numbers exhibit the following features: (1) When periodically rotating two blades of equal lengths, the local maximum of AFSRs, 959,915, occurs in the case of $L_1 = L_2 = \pi/2$. On the other hand, the greatest AFSR, 2,501,247, is achieved by using blades of lengths

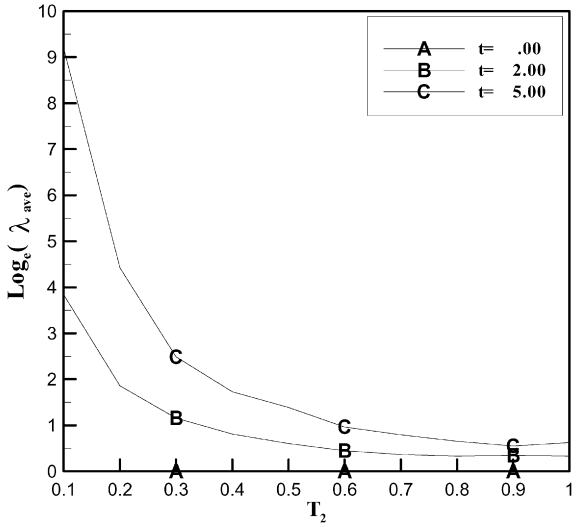

Fig. 6. Time variations of the Averaged Fluid Stretch Rate (AFSR) for flows with blade lengths $L_1 = \pi/4$, $L_2 = \pi/4$.

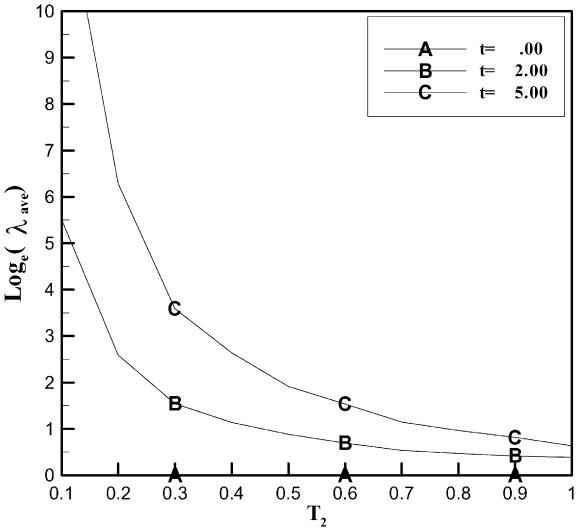

Fig. 7. Time variations of AFSRs for flows with blade lengths $L_1 = \pi/4$, $L_2 = \pi/2$.

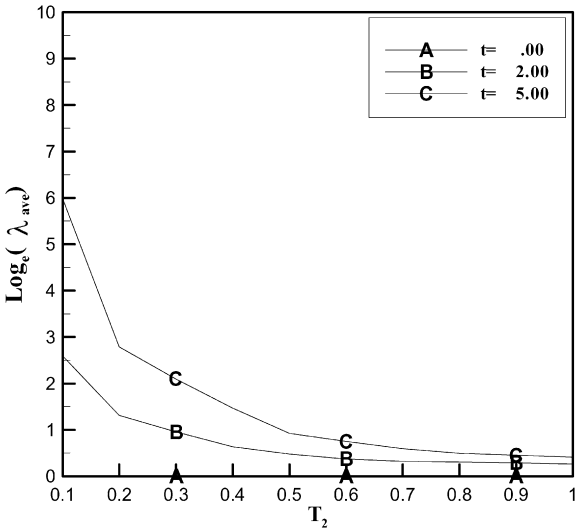

Fig. 8. Time variations of AFSRs for flows with blade lengths $L_1 = \pi/4$, $L_2 = 3\pi/4$.

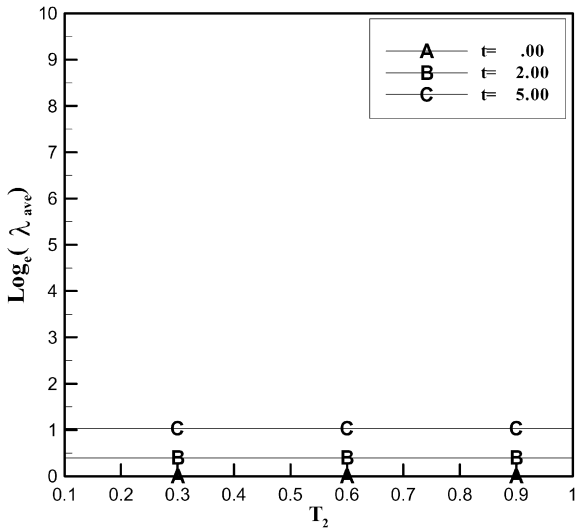

Fig. 9. Time variations of AFSRs for flows with blade lengths $L_1 = \pi/4$, $L_2 = \pi$ (one moving blade).

Table 1
The averaged fluid stretch-rates of flows obtained for various blade lengths L_1 and L_2, operated at periods $T_1 = 1$, $T_2 = 0.1$, and examined at time $t = 5$

L_2	L_1			
	$\pi/4$	$\pi/2$	$3\pi/4$	π *
$\pi/4$	9,834	7,275	15,553	13,841
$\pi/2$	404,052	959,915	2,501,247	1,125,908
$3\pi/4$	395	807	1,105	2,047
π*	2.8	4.3	2.6	1

* The blade with a length of π is kept stationary, leaving only one of the two blades free to rotate.

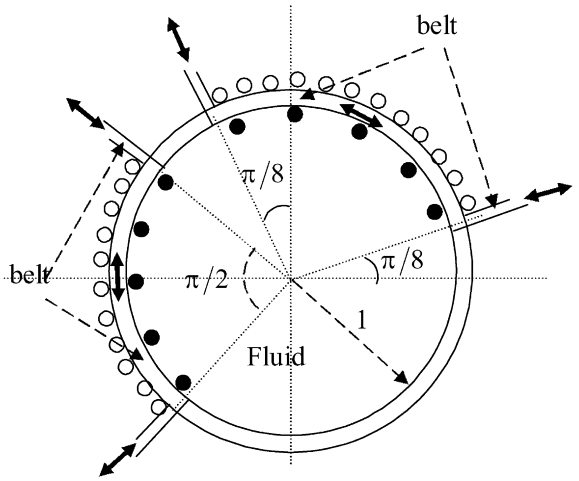

Fig. 10. Sketch of circular cavity with two belts generating the greatest averaged fluid stretch-rate (disturbances introduced by the inner slender cylinders to flow field computations are neglected).

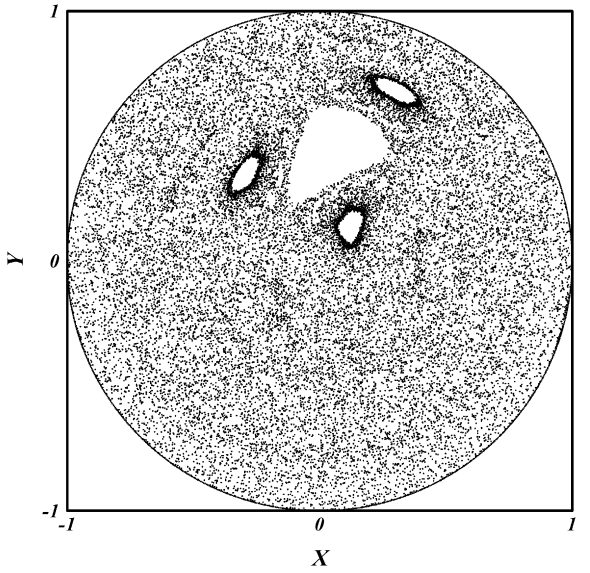

Fig. 11. The Poincaré section for flow with rigid blades of lengths $L_1 = 3\pi/4$, $L_2 = \pi/2$, operated at periods $T_1 = 1.0$, $T_2 = 0.1$.

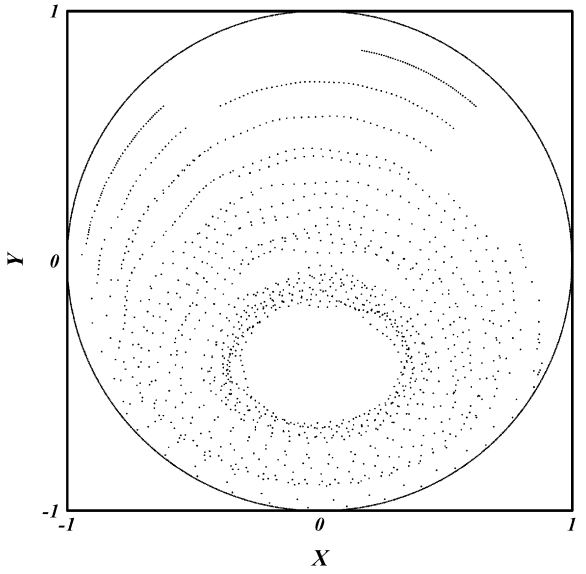

Fig. 12. The Poincaré section for flow with rigid blades of lengths $L_1 = 3\pi/4$, $L_2 = \pi$, operated only for the first blade at period $T_1 = 1.0$.

$L_1 = 3\pi/4$ and $L_2 = \pi/2$. In this mixing protocol, the longer blade has the longer period. (2) It is interesting to find that the AFSR decreases largely to 807, when the blades take lengths $L_1 = \pi/2$ and $L_2 = 3\pi/4$. This suggests that longer blades rotated with longer periods are favorable to stirring of fluid. However the AFSRs of the cavity flows with the blade lengths $\pi/2$ and $\pi/4$ violate the prediction. The AFSR is 7275 for ($L_1 = \pi/2$, $L_2 = \pi/4$) and 404,052 for ($L_1 = \pi/4$, $L_2 = \pi/2$). (3) As mentioned previously, when a single blade is used, higher AFSRs can be generated by rotating the blade under the shorter period 0.1 ($L_1 = \pi$) instead of the longer period 1 ($L_2 = \pi$). Moreover, the fluid mixer with a moving blade length of $\pi/2$ yields a local maximum AFSR of 1,125,908.

The stirring of fluid obtained with the present fluid mixer can now be compared with previous results for the belt-driven cavities (Hwu [15]). Fig. 10 shows the circular cavity flow that has yielded the greatest AFSR in the

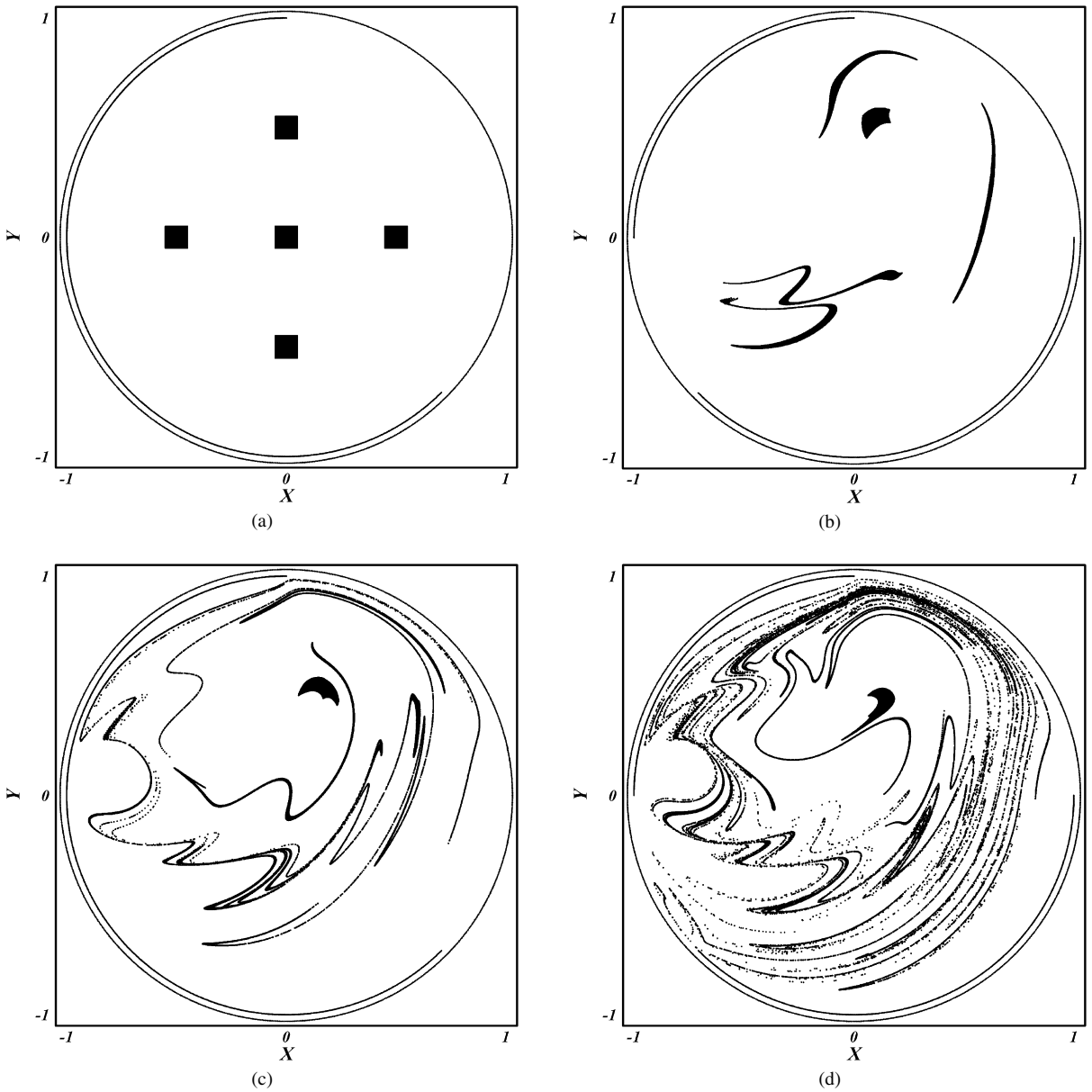

Fig. 13. Successive deformations of fluid blobs in flow generated by rigid blades of lengths $L_1 = 3\pi/4$, $L_2 = \pi/2$, operated at periods $T_1 = 1$, $T_2 = 0.1$, and examined at the following times: (a) $t = 0$, (b) $t = 0.5$, (c) $t = 1$, (d) $t = 1.5$, (e) $t = 5$.

previous studies (Hwu [15]). The rotating angular velocities of the belts are chosen as $\Omega_1(t) = +2\sin^2(\pi t/3)$ and $\Omega_2(t) = -2\cos^2(\pi t/3)$, respectively (Hwu [15]). It is surprise to find that, when $t = 5$, the value of the AFSR is about equal to 3. Even at time $t = 30$, the AFSR is about only 960. These values are much lower than the value of 2,501,247 obtained for the greatest stretch-rate in the present investigation. The proposed new mixer in which rigid blades are used instead of flexible belts is thus formed to be much more efficient at stirring the fluid.

To further document the results, the Poincaré sections of two flows are constructed as follows. The first flow chosen takes parameters $L_1 = 3\pi/4$, $T_1 = 1.0$ and $L_2 = \pi/2$, $T_2 = 0.1$ that generate the greatest AFSR of 2,501,247. For contrast, the second flow takes parameters $L_1 = 3\pi/4$, $T_1 = 1.0$ and $L_2 = \pi$ which yield the smallest AFSR of 2.6. To create the Poincaré sections, 28 fluid points were traced and the successive positions were recorded at times $t = nT_2$ ($n =$ integer) over a time span of 5. Fig. 11 shows the result for the first flow. In this case, the fluid was mixed by two blades of different lengths actuated at different oscillation periods, with one period ten times larger than the other.

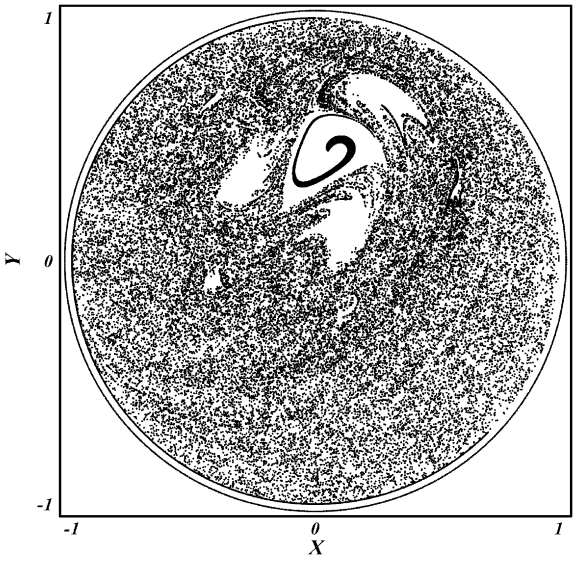

(e)

Fig. 13 (*continued*).

Because one of the blades was rapidly moved back and forth, along the cavity wall, the fluid had a chance to be stirred completely. Accordingly, the Poincaré section shows that the dots spread extensively throughout most of the domain. It can be noted that there are period-3 islands and a "white hole" in the chaos sea. Within these regimes, the fluids remain undertaking regular motions. As predicted by KAM theory, mass exchanges do not occur on the boundaries between the isolated areas and the chaotic region. Fig. 12 shows the corresponding Poincaré section for the second flow. In this case, the blade actuated at a shorter period was turned off, leaving only one slowly rotating blade to mix the fluid. The stirring of fluid is poor and the picture shows dots aligned along smooth trajectories with only slight perturbations.

Besides the AFSRs and the Poincaré sections, successive deformations of several fluid blobs (Fig. 13(a)) can be traced to clearly depict the detailed processes of the stirring of fluid. By means of this, one can gain a better perspective regarding the kinematical features of the stirring of fluid and check whether the fluid is stirred completed, when the fluid have high AFSRs and the fluid points have been widely spread on the Poincaré sections. Fig. 13 represents the motions of five fluid blobs for the flow examined previously using a Poincaré section in Fig. 11 and for which the AFSR is the greatest. As time proceeds to 0.5, Fig. 13(b) displays that the fluid blobs experience rotations and stretchings by the actions of the two moving blades. The fluid blobs undergo meandering motions due to the periodic oscillations of the blades. As required for mass conservation of the incompressible fluid, the area of each blob does not vary. When $t = 1$, Fig. 13(c) shows four of the fluid blobs being extensively stretched along some directions. Because the fluid flows in a closed cavity, these blobs are subject to repeated folding. The remaining blob, however, does not exhibit such severe deformations. Fig. 13(d) shows the corresponding deformations at $t = 1.5$. In this diagram, fluid has been stirred to a large extent. The area explored by the marked fluids increases largely as compared with those at the previous times. This can be interpreted to reflect the exponential grows of the fluid stretch-rates. At $t = 5$, Fig. 13(e) reveals a picture in which the fluid has undergone a nearly complete stirring. Four of the fluid blobs have been extensively stretched, bended and folded, and have been dispersed throughout the circular flow domain. Less thorough stirring is however observed for one of the blobs, initially located in the "white hole" (Fig. 11), and which undergoes regular motions. For the second flow, the evolution of the fluid blobs at $t = 5$ is shown in Fig. 14. This is the flow configuration for which the Poincaré section was plotted in Fig. 12 and for which the AFSR is the smallest. With only one of the blades rotated, the fluid experiences only slight perturbations within the circular cavity, leading to a poor stirring efficient.

Fig. 15 displays the stirring of a fluid filament in the cavity for which the AFSR obtained is the greatest. Fig. 15(a) shows the initial position of the fluid tracer and thus proceeded as in Fig. 15(b) at $t = 0.5$. In this short time, the fluid filament was heavily stretched and folded, due to the oscillations and to the influence of the nearby boundaries. In the

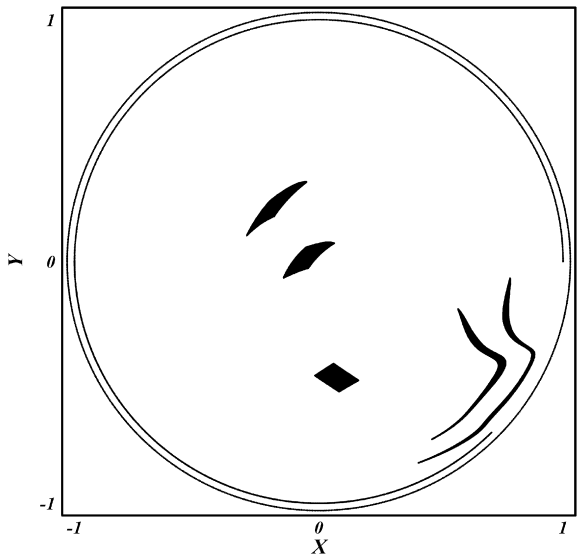

Fig. 14. Deformations of fluid blobs in flow generated by rigid blades of lengths $L_1 = 3\pi/4$, $L_2 = \pi$, operated only for the first blade at period $T_1 = 1$, and examined at the time $t = 5$.

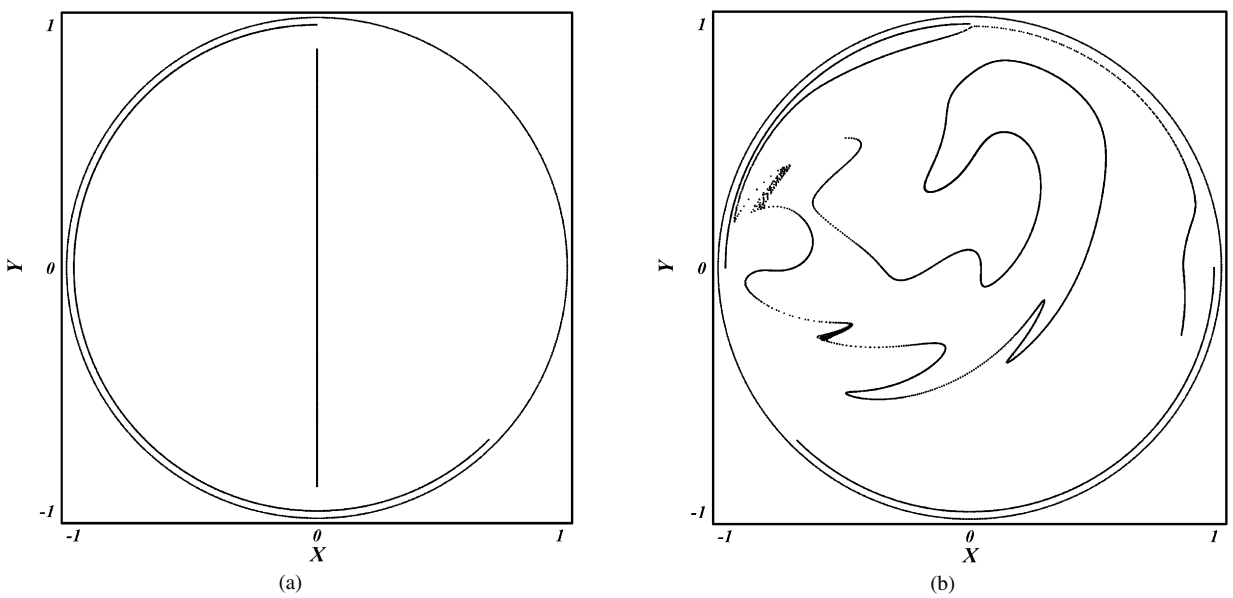

Fig. 15. Successive deformations of fluid filament in flow generated by rigid blades of lengths $L_1 = 3\pi/4$, $L_2 = \pi/2$, operated at periods $T_1 = 1$, $T_2 = 0.1$, and examined at the following times: (a) $t = 0$, (b) $t = 0.5$.

viscous fluid flow, any two particles initially located at a small distance from each other undergo repeated separation and approach moves. Accurate simulations of the deformation processes for a large number of fluid particles are expensive both in time and in memory. Therefore, it is difficult to construct a global picture for the stirring of fluid. If one wants to know how the fluid can attain a larger overall stretch-rate, Table 1 can be consulted. To construct a rough draft, 37 fluid blobs initially located as shown in Fig. 16(a) were used. The simulations were also performed on the mixer resulting in the greatest fluid stretch-rate. When the stirring is conducted over a time span of 2, the fluid is observed to be nearly completely mixed, as documented in Fig. 16(b). The stirring develops much like the process described earlier in relation to Fig. 13.

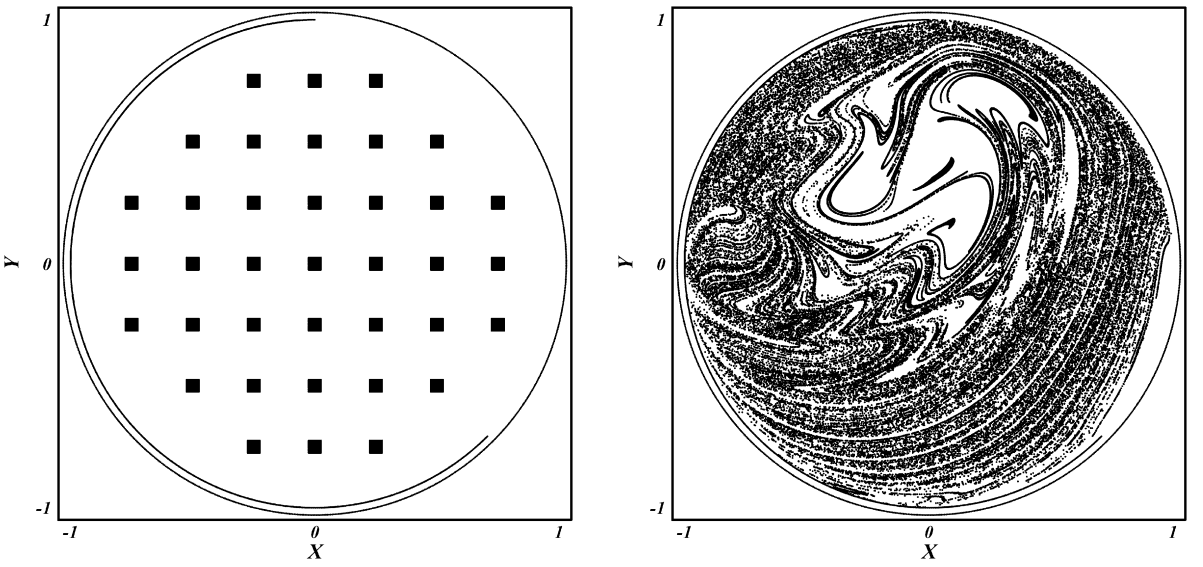

Fig. 16. Successive deformations of 37 fluid blobs in flow generated by rigid blades of lengths $L_1 = 3\pi/4$, $L_2 = \pi/2$, operated at periods $T_1 = 1$, $T_2 = 0.1$, and examined at the following times: (a) $t = 0$, (b) $t = 2$.

4. Conclusions

The present investigation proposed a new fluid mixer that can be realistically constructed and operated in experiments. By using rigid blades, the proposed devices improve an earlier device based on flexing belts, and generates much higher averaged fluid stretch-rates in a short time. Furthermore, the fluid can be mixed completed by carefully choosing the dimensions and operating parameters of the blades installed within the cylindrical container. Such through mixing was found to be impossible to attain in the configurations considered previously. By choosing suitable lengths and oscillation periods for the blades, the fluid may be deformed to averaged stretch-rates taking very large magnitudes of up to 2,501,247.

Acknowledgements

The present study was supported by the National Science Council of the Republic of China under Research Grants NSC-91-2211-E-267-003. Thanks are extended to Dr. H. Capart for discussion of an earlier draft of the present manuscript.

References

[1] J.M. Ottino, The Kinematics of Mixing: Stretching, Chaos, and Transport, Cambridge University Press, Cambridge, 1989.
[2] H. Aref, S. Balachandar, Chaotic advection in a Stokes flow, Phys. Fluids 29 (11) (1986) 3515–3521.
[3] J. Chaiken, R. Chevray, M. Tabor, Q.M. Tan, Experimental study of Lagrangian turbulence in a Stokes flow, Proc. Roy. Soc. London Ser. A 408 (1986) 165–174.
[4] P.D. Swanson, J.M. Ottino, A comparative computational and experimental study of chaotic mixing of viscous fluids, J. Fluid Mech. 213 (1990) 227–249.
[5] P. Dutta, R. Chevray, Effect of diffusion on chaotic advection in Stokes flow, Phys. Fluids A 3 (5) (1991) 1440.
[6] W.L. Chien, H. Rising, J.M. Ottino, Laminar mixing and chaotic mixing in several cavity flows, J. Fluid Mech. 170 (1986) 355–377.
[7] C.W. Leong, J.M. Ottino, Experiments on mixing due to chaotic advection in a cavity, J. Fluid Mech. 209 (1989) 463–499.
[8] M. Liu, R.L. Peskin, F.J. Muzzio, C.W. Leong, Structure of the stretching field in chaotic cavity flows, AIChE J. 40 (8) (1994) 1273–1286.
[9] S.C. Jana, M. Tjahjadi, J.M. Ottino, Chaotic mixing of viscous fluids by periodic changes in geometry: baffled cavity flow, AIChE J. 40 (11) (1994) 1769–1781.
[10] T.Y. Hwu, D.L. Young, Y.Y. Chen, Chaotic advections for Stokes flows in circular cavity, ASCE J. Eng. Mech. 123 (8) (1997) 774–782.
[11] L.D. Landau, E.M. Lifshitz, Fluid Mechanics, Pergamon, Oxford, 1959.
[12] A.N. Tychonov, A.A. Samarski, Partial Differential Equation of Mathematical Physics, 1, Holden-Day, San Francisco, 1964.

[13] P.R. Garabedian, Partial Differential Equations, John Wiley and Sons, New York, 1964.
[14] R.D. Mills, Computing internal viscous flow problem for the circle by integral method, J. Fluid Mech. 79 (3) (1977) 609–624.
[15] T.Y. Hwu, Fluid stirrings in a circular cavity with various driven boundaries, Eur. J. Mech. B Fluids 25 (2) (2006) 192–203.